Title: Spatio-temporal regulation of cell motility and its fitness effect in a surface-attached bacterial community.

Author: Emrah Şimşek[1,5], Emma Dawson[1], Philip N. Rather[2,3,4], Minsu Kim[1,2,*].

[1] Department of Physics, Emory University, Atlanta, GA, 30322. U.S.A.

[2] Graduate Division of Biological and Biomedical Sciences, Emory University, Atlanta, GA, 30322. U.S.A.

[3] Department of Microbiology and Immunology, Emory University, Atlanta, GA, 30322. U.S.A.

[4] Research Service, Atlanta VA Medical Center, Decatur, GA, 30033. U.S.A.

[5] Present address: Department of Biomedical Engineering, Duke University, Durham, NC 27708. U.S.A.

*To whom correspondence should be addressed. Tel: 404-727-8037; FAX: 404-727-0873; Email: minsu.kim@emory.edu

Abstract

On a surface, microbes grow into a multi-cellular community. When a community becomes densely populated, cells migrate away to expand it. How microbes regulate surface motility to optimize the expansion remains poorly understood. Here, we characterized surface motility of *Proteus mirabilis*. *P. mirabilis* is well known for its extraordinary ability to expand its colony rapidly on a surface. Cursory visual inspection of an expanding colony suggests partial migration, i.e., one fraction of a population migrates while the other is sessile. Quantitative real-time imaging with a microscope reveals that this migration pattern is determined by temporally and spatially dynamic regulation of cell motility. Further analyses reveal that this spatio-temporal regulation is well accounted for by nutrient-dependent repression

of cell motility by the Rcs system. Alleviating this repression increases the colony expansion speed but results in a rapid drop in the number of viable cells, lowering population fitness. These findings collectively demonstrate a fundamental trade-off underlying bacterial colonization of a surface, and how Rcs dynamically regulates cell motility to increase the fitness of an expanding bacterial population.

Introduction

In nature, bacteria often grow on a surface and develop a multi-cellular community (1, 2). When a community becomes densely populated, cells migrate away to expand their community (3). This process poses significant industrial and medical challenges because it leads to the spread of biofouling and chronic infections (4-6). However, several fundamental questions remain unanswered. Specifically, dispersal is mediated by phenotypic (or genotypic) "variants" (7). What are the ecological factors that drive the generation of these migratory variants? What are the signal transduction pathways that are used to sense these ecological factors and trigger the generation of migratory variants?

These questions are not limited to bacteria, as migration is a fundamental process of living organisms (8, 9). Migration results in a profound change in population density in space and time, altering local ecological interactions, e.g., species competition and spread of invasive species (10-15). Interestingly, a wide variety of organisms exhibit partial migration, where a fraction of a population moves away while the rest remains sessile. This type of migration has been documented for mammals, birds, fish, amphibians, and insects (16). However, how and why a population diversifies when expanding its territory is poorly understood. While several theoretical studies have proposed potential benefits of partial migration (17-19), they have not been experimentally tested.

In this study, we characterized the surface expansion of bacterial communities in the context of partial migration. We chose *Proteus mirabilis* as a model system because of its superior ability to expand its community (20). This superior ability underlies the pathogenesis of this bacterium as it enables *P. mirabilis* cells to reach across the urethra and colonize the bladder and kidneys, and leads to rapid surface fouling of newly inserted catheters (21-25). This superior ability can be visualized on agar surfaces in a laboratory, as *P. mirabilis* can expand its colony on high agar concentrations (>1 %), which are too stiff for other model bacteria including *Escherichia coli* or *Bacillus subtilis* (9, 26-28). Here, we investigated the expansion dynamics of *P. mirabilis* to identify a regulatory mechanism and strategy for its surface colonization.

Materials and Methods

Bacterial growth conditions.

P. mirabilis ATCC 7022 and its derivatives were used; see Supplementary Table 1 for the strain information. Liquid cultures were prepared in Luria-Bertani (LB) broth at 37°C with shaking at 200 rpm. Cells were inoculated from an -80°C frozen stock a day before an experiment and grown overnight. A small volume of an overnight culture was suspended in fresh medium to prepare an experimental culture. Cells were grown in an experimental culture for at least five doubling before measurements were made as described in the text. Cell density was determined by quantifying the optical density at 600 nm wavelength (OD_{600}) using a Genesys20 spectrophotometer (Thermo Fisher) with a standard cuvette (16.100-Q-10/Z8.5; Starna Cells). See Supplementary Methods for further details.

Microscopy and image analysis.

The cells were imaged using an inverted microscope (Olympus IX83P2Z). The microscope was controlled by the MetaMorph software (Molecular Devices) and housed in a microscope incubator (InVivo Scientific) which maintained the temperature of samples at 37°C during the experiments. Images were captured using a Neo 5.5 scientific CMOS camera (Andor). Images were analyzed using MicrobeJ, a freely available plug-in for ImageJ, or a custom-built MATLAB software. See Supplementary Methods for further details.

Results

Expansion dynamics of a surface-attached *P. mirabilis* colony.

We studied the expansion of a wild-type (WT) *P. mirabilis* population by depositing an inoculum droplet on a surface of an LB medium solidified with ~2% agar. When deposited on a surface, a WT *P. mirabilis* population first grows in its original inoculum zone and forms a colony; see Supplementary Fig. 1a. Only after a colony reaches a high cell density (~10^9 cells/cm^2), it initiates migration; Supplementary Fig. 1b and caption. Migration is visualized by the appearance of a faint halo beyond the distinct boundary of a

densely-packed parental colony (Fig. 1A). Throughout population migration, the boundary of the parent colony remains stationary and distinct, suggesting that a majority of cells remain in the parental colony.

We then directly determined the migrating fraction in a colony. *P. mirabilis* cells migrate on stiff surfaces by differentiating to the hyperelongated and hyperflagellated phenotype (20). Cells exhibiting this motile phenotype can migrate across a surface through a process known as swarming (9, 26-29). We and others have shown that differentiation occurs in a subpopulation of cells (30, 31). Here, we quantified the fraction of this subpopulation by harvesting the entire population and determining the number of hyperelongated cells with a microscope (see Supplementary Fig. 2 and Methods for detail). We found that only ~1% of cells exhibited the motile phenotype (Fig. 1C, green).

Severe repression of migration in the inner region of an expanding colony.

How and why is the migratory fraction kept at such a low level? We first sought to unravel a regulatory mechanism controlling the migratory fraction by characterizing the spatio-temporal dynamics of the motile phenotype. The *flhDC* gene encodes the master regulator for differentiation into the motile phenotype (32, 33). We constructed a transcriptional fusion of the *flhDC* and green fluorescent protein (*gfp*) genes and tracked *flhDC* expression by monitoring GFP intensity in a colony over time. We found that as a colony matures, GFP intensity increases in cells at the colony edge (Supplementary movie 1 left panel). These GFP-bright cells differentiate to the motile phenotype and migrate away from the parental colony. In the inner region of the colony, however, GFP intensity remained low, and no differentiation occurred (Supplementary Movie right panel). This severe repression of motility in the inner region explains how a large fraction of a population remains sessile in an expanding colony.

This movie also revealed a narrow, distinct band of cells at the colony edge, where the most of GFP-bright cells were located (Supplementary Movie left panel). The formation of this band can be described by the coffee ring effect, a well-known physical phenomenon caused by capillary flow which pushes particles to the edge of a droplet (34). This effect was also frequently observed in previous studies of bacterial colony formation (35, 36). We wondered whether the formation of this band is responsible for

the preferential increase in GFP intensity at the colony edge. To avoid this effect, we started colonies from single cells by diluting and spreading an inoculum droplet over a large area of agar surface. Colonies originating from single cells did not exhibit such bands, and yet GFP intensity was still preferentially higher at the colony edge (Fig. 2A).

Having characterized the spatial dynamics of *flhDC* expression, we then focused on its temporal dynamics. We found that as a colony grows, the GFP intensity in the colony center increases initially (left of the grey region in Fig. 2B). This intensity increase is likely due to an increase in cell density, rather than due to specific regulation, as we observed a similar fluorescence increase in a growing colony of cells *constitutively* expressing fluorescent proteins (Supplementary Fig. 3A). What is striking is that GFP intensity drops abruptly at 180 min (grey region in Fig. 2B), indicating the repression of *flhDC* expression. Importantly, simultaneous measurements of colony size reveal that the onset of this repression occurs concurrently with the onset of colony growth slowdown (Supplementary Fig. 4).

Nutrient depletion leads to the repression of cell motility.

This concurrent occurrence suggests that colony growth slowdown and repression of *flhDC* expression share the same underlying mechanism. Previous studies of colony growth on agar surface have shown that cells in the inner region of a colony experience nutrient depletion (37-39). Due to nutrient depletion, cells located just several cell lengths inside the colony edge can already exhibit slower growth, especially in a mature colony (40, 41). This is consistent with the results from our control experiments with stable and degradable GFPs. In our previous experiments, we tracked colony growth of a strain that constitutively expressed stable GFP. We found that the GFP intensity is significantly higher at the colony center than edge, due to higher cell density (Supplementary Fig. 3B). We repeated this experiment using a strain that constitutively expresses a *degradable* GFP. The fluorescence intensity of degradable GFP is directly related to the growth rate of cells, and thus it has been used to detect slow-growing cells in a liquid culture or colony (40, 42) . In contrast to our findings with stable GFP, the fluorescence intensity of degradable GFP was significantly lower in the colony center than edge (Supplementary Fig. 5B),

indicating slow cell growth in the center. These findings by us and others collectively suggest that nutrient depletion in the colony center is responsible for an overall slowdown of colony growth. Then, one likely explanation for the observed concurrent occurrence of colony growth slowdown and repression of *flhDC* expression is that nutrient depletion also causes this repression.

Testing nutrient-dependent repression of cell motility.

We tested this hypothesis, i.e., nutrient-dependent repression of *flhDC* expression, through several independent experiments. First, we lowered nutrient concentration in the external environment. In previous experiments, we used an agar solidified with 1× LB. When we used 0.2× LB, we observed a more severe decrease in *flhDC* expression in the colony center (blue squares in Fig. 2C), supporting nutrient-dependent repression of *flhDC* expression. (Note that the *flhDC* expression continued to decrease at the end of the experiment, but it was difficult to continue the measurement because of the interference by motile cells generated from other colonies.)

We further tested our hypothesis by investigating a potential molecular factor mediating this repression of *fhlDC* expression. To do so, we searched for mutants that do not exhibit this repression. In the WT strain, this repression is manifest in its migration pattern as discussed above; the boundary of a parental colony remains stationary and distinct during expansion, which indicates that a majority of cells do not participate in migration (Fig. 1). (Migration is visualized by a faint halo around the fixed colony boundary.) During our transposon mutagenesis screening, we identified mutants that showed different expansion dynamics: they shifted the entire colony boundary outward during migration (Fig. 1B and Supplementary Fig. 6). We found that these mutants have the transposon insertion in the *rcsC* or *rcsB* genes, two components of the Rcs phosphorelay system (43-45). As transposon insertion might be unstable, we performed clean knockout of these genes (See Supplementary Methods). These mutants exhibited the same, outward shift of the colony boundary. We next tracked the radius of the population edge, which showed that the edge moves faster in the mutant colony than WT colony (Supplementary Fig. 7).

The observed, robust expansion of the colony boundary exhibited by these mutants suggests that a large fraction of the population migrates. We confirmed this by quantifying the fraction of cells expressing the motile phenotype in a Δ*rcsC* population. We found that ~50% of a population participates in migration (Fig. 1C, red), a fraction significantly higher than the ~1% observed in the WT population (Fig. 1C, green). Importantly, this large increase in the migratory fraction suggests that *rcsC* knockout relieved the repression of *flhDC* expression (note that *flhDC* is the master regulator for differentiation into the motile phenotype (32, 33)). This is consistent with our and others' previous findings that *flhDC* is a member of the Rcs regulon (43-49).

To examine whether this repression by Rcs is nutrient-dependent, we first compared the spatio-temporal dynamics of *flhDC* expression between the Δ*rcsC* and WT strains. Our previous temporal measurements showed that the WT strain exhibited an abrupt repression of *flhDC* expression in the colony center, where nutrient depletion is severe (grey region in Fig. 2C). When we repeated this experiment with the Δ*rcsC* strain, however, we did not observe such a repression; see a monotonic increase in *flhDC* expression in the regime where WT exhibits a decreased expression (grey region in Fig. 2D). This difference was also evident in raw fluorescence images of their colonies. In the WT colony, *flhDC* expression is significantly lower in the colony center than edge (Fig. 2A). In the mutant colony, *flhDC* expression is uniform across the colony (Supplementary Fig. 8). These findings support that the Rcs system mediates nutrient-dependent repression of *flhDC* expression.

We further tested this nutrient dependence by examining *flhDC* expression at different distances away from the colony center. In contrast to the colony center, cells near the colony edge have access to nutrients diffusing from the surrounding environment (40, 41). If *flhDC* repression is indeed nutrient-dependent and mediated by the Rcs system, *flhDC* expression near the edge must not decrease at increasing colony size. This prediction is supported by our finding, which showed that at 0.6 times the colony radius (Fig. 2E) and larger (Supplementary Fig. 9), *flhDC* expression does not decrease as a colony grows but remains largely constant in the WT strain (green symbols). We found a similar pattern

in the Δ*rcsC* strains (red symbols). This similarity between WT and Δ*rcsC* strains at the colony edge (but not in the center) further supports that *flhDC* repression by Rcs is nutrient-dependent.

We next used a liquid culture to further examine the nutrient-dependence of Rcs-mediated *flhDC* repression. An advantage of a liquid culture is that it can be shaken and well-mixed, providing a better control for a nutrient condition. We found that *flhDC* expression in Δ*rcsC* and WT strains grown in 1× LB liquid cultures was comparable (Fig. 3A). In a lower nutrient condition (0.2× LB), however, *flhDC* expression in the Δ*rcsC* strain was more than 20-fold higher than that in WT, which, again, supports our hypothesis that the repression of *flhDC* expression by Rcs is nutrient-dependent.

Fitness advantage of the WT (*rcsC*+) strain.

A Δ*rcsC* colony expands faster than a WT colony (Supplementary Fig. 7), because it has a much higher fraction of migratory cells (Fig. 1C). Then, what is the advantage of keeping the migratory fraction low? To address this question, we compared the fitness of WT and Δ*rcsC* strains. Specifically, we spread cells on an agar surface and evaluated the biomass yield by measuring $OD_{600} \times$ ml and cell viability by counting colony forming units (CFU) over time. We used 0.2× LB agar because the repression is pronounced in a low-nutrient environment (Fig. 2C). We found that the Δ*rcsC* strain produced less biomass than WT in a given territory, although the difference is marginal (Fig. 3B, open symbols). Importantly, the Δ*rcsC* strain exhibited a noticeably steeper decrease in cell viability than WT (Fig. 3B, solid symbols), revealing a trade-off between population expansion and viability.

Discussion

Our quantitative real-time imaging uncovered intricate spatio-temporal dynamics of cell motility governing partial migration of a population. We then systematically analyzed the dynamics (colony center vs. edge, WT vs. Δ*rcs* strains, high vs. low nutrient levels on agar surface and in liquid culture), which revealed an important role of the Rcs system in these dynamics. The Rcs system is widespread in the *Enterobacteriaceae* family (50) and known to regulate a wide range of cellular functions including

capsular polysaccharide or colanic acid synthesis, cell envelope maintenance, cell division and virulence (51). However, physiological cues inducing this system and its functional role in colonizing territories were unclear. Our present work reveals that nutrient-dependent repression of *flhDC* expression by this system leads to intricate spatio-temporal dynamics of cell motility in an expanding population, thereby having a major impact on the surface colonization pattern.

We additionally found that this Rcs-mediated repression of cell motility provides a substantial fitness advantage. Swimming in liquid costs about 2% of metabolic budget in bacteria (52). The cost of surface motility (swarming) has not been measured, but is thought to be much greater (26, 53). Consistent with this view, we found that *P. mirabilis* cells that are actively moving on a surface reproduce at a very low rate or do not reproduce (Supplementary Fig. 10), indicating a severe cost of surface motility. This cost is likely more burdensome in nutrient-limiting conditions, where cells already suffer from a limited metabolic budget. Our studies show that, although inducing migration in the face of this cost (Δ*rcs* strain) does lead to faster population expansion, it severely impairs population fitness. Nutrient-dependent repression of cell motility by Rcs can minimize this cost in nutrient-limited cells while enabling migration only for a small number of privileged cells that have access to nutrients. This mode of partial migration can provide one mechanism to mediate a trade-off, helping a population maintain its fitness during expansion, thereby facilitating surface colonization.

Interestingly, previous studies suggest an additional mechanism for fitness advantage. RpoS is a general stress sigma factor that is widely present in *Enterobacteriaceae* (54). In our previous studies with *E. coli*, we have shown that in nutrient-limiting conditions, RpoS plays a critical role in conserving a limited metabolic budget for starvation survival (55). Such a protective role of RpoS is well documented for a wide variety of other bacterial species (54). Interestingly, recent studies have found that RpoS expression is induced by Rcs (56, 57). Therefore, Rcs not only represses cell motility in the nutrient-limited region (as discussed in the preceding paragraph) but also is expected to induce the expression of the important stress sigma factor (RpoS). This two-pronged response is likely to contribute to fitness advantage

conferred by Rcs. Importantly, migration is expected to incur a high cost of dispersal in other organisms as well, impairing their reproduction rate and survival (58-60). A similar strategy could be used in these organisms to optimize territory expansion.

Our findings also shed new light on a surface-attached microbial community, biofilm. Surface motility is known to have a dramatic effect on biofilm formation (27, 61). We found that motility is strongly repressed by Rcs in a dense region of a colony (Fig. 2A), which ensures that a majority of cells remain sessile within the colony. Due to this repression, the boundary of a parental colony remains distinct and stationary during expansion (Fig. 1A), which enables the maintenance of the original densely-packed community. The same mechanism is likely at play in a biofilm, where *rcs* ensures the formation of a robust biofilm by inhibiting premature dispersal. This is consistent with previous studies of *E. coli*, *P. mirabilis*, and other bacteria, which have shown that *rcs* deletion leads to the formation of defective biofilms (44, 62, 63).

Acknowledgement: We thank Kirill Korolev and Ashish George for helpful discussions.

Conflict of Interest

The authors declare no competing financial interests

Reference

1. Flemming H-C, Wingender J, Szewzyk U, Steinberg P, Rice SA, Kjelleberg S. Biofilms: an emergent form of bacterial life. Nature Reviews Microbiology. 2016;14(9):563-75.

2. Nadell CD, Xavier JB, Foster KR. The sociobiology of biofilms. FEMS microbiology reviews. 2009;33(1):206-24.

3. Rumbaugh KP, Sauer K. Biofilm dispersion. Nature Reviews Microbiology. 2020;18(10):571-86.

4. Costerton JW, Stewart PS, Greenberg EP. Bacterial biofilms: a common cause of persistent infections. Science. 1999;284(5418):1318-22.

5. Drenkard E, Ausubel FM. Pseudomonas biofilm formation and antibiotic resistance are linked to phenotypic variation. Nature. 2002;416(6882):740-3.

6. de Carvalho CCCR. Marine Biofilms: A Successful Microbial Strategy With Economic Implications. Frontiers in Marine Science. 2018;5(126).

7. McDougald D, Rice SA, Barraud N, Steinberg PD, Kjelleberg S. Should we stay or should we go: mechanisms and ecological consequences for biofilm dispersal. Nature Reviews Microbiology. 2012;10(1):39-50.

8. Nathan R, Getz WM, Revilla E, Holyoak M, Kadmon R, Saltz D, et al. A movement ecology paradigm for unifying organismal movement research. Proceedings of the National Academy of Sciences. 2008;105(49):19052-9.

9. Yan J, Monaco H, Xavier JB. The Ultimate Guide to Bacterial Swarming: An Experimental Model to Study the Evolution of Cooperative Behavior. Annual review of microbiology. 2019;73(1):293-312.

10. Gokhale S, Conwill A, Ranjan T, Gore J. Migration alters oscillatory dynamics and promotes survival in connected bacterial populations. Nature communications. 2018;9(1):5273.

11. Hallatschek O, Fisher DS. Acceleration of evolutionary spread by long-range dispersal. Proceedings of the National Academy of Sciences of the United States of America. 2014;111(46):E4911-9.

12. Birzu G, Hallatschek O, Korolev KS. Fluctuations uncover a distinct class of traveling waves. Proceedings of the National Academy of Sciences. 2018;115(16):E3645-E54.

13. Ping D, Wang T, Fraebel DT, Maslov S, Sneppen K, Kuehn S. Hitchhiking, collapse, and contingency in phage infections of migrating bacterial populations. The ISME journal. 2020;14(8):2007-18.

14. Chen L, Noorbakhsh J, Adams RM, Samaniego-Evans J, Agollah G, Nevozhay D, et al. Two-Dimensionality of Yeast Colony Expansion Accompanied by Pattern Formation. PLoS computational biology. 2014;10(12):e1003979.

15. Patra P, Kissoon K, Cornejo I, Kaplan HB, Igoshin OA. Colony Expansion of Socially Motile Myxococcus xanthus Cells Is Driven by Growth, Motility, and Exopolysaccharide Production. PLoS computational biology. 2016;12(6):e1005010.

16. Chapman BB, Brönmark C, Nilsson J-Å, Hansson L-A. The ecology and evolution of partial migration. Oikos. 2011;120(12):1764-75.

17. Lundberg P. Partial bird migration and evolutionarily stable strategies. Journal of theoretical biology. 1987;125(3):351-60.

18. Kokko H. Directions in modelling partial migration: how adaptation can cause a population decline and why the rules of territory acquisition matter. Oikos. 2011;120(12):1826-37.

19. Singh NJ, Leonardsson K. Partial Migration and Transient Coexistence of Migrants and Residents in Animal Populations. PloS one. 2014;9(4):e94750.

20. Armbruster CE, Mobley HLT. Merging mythology and morphology: the multifaceted lifestyle of Proteus mirabilis. Nature Reviews Microbiology. 2012;10:743.

21. Schaffer JN, Pearson MM. Proteus mirabilis and Urinary Tract Infections. Microbiology spectrum. 2015;3(5):10.1128/microbiolspec.UTI-0017-2013.

22. Jones BV, Young R, Mahenthiralingam E, Stickler DJ. Ultrastructure of Proteus mirabilis swarmer cell rafts and role of swarming in catheter-associated urinary tract infection. Infect Immun. 2004;72(7):3941-50.

23. Li X, Zhao H, Lockatell CV, Drachenberg CB, Johnson DE, Mobley HL. Visualization of Proteus mirabilis within the matrix of urease-induced bladder stones during experimental urinary tract infection. Infect Immun. 2002;70(1):389-94.

24. Stickler DJ. Bacterial biofilms in patients with indwelling urinary catheters. Nature clinical practice Urology. 2008;5(11):598-608.

25. Jacobsen SM, Stickler DJ, Mobley HLT, Shirtliff ME. Complicated Catheter-Associated Urinary Tract Infections Due to Escherichia coli and Proteus mirabilis. Clinical Microbiology Reviews. 2008;21(1):26-59.

26. Harshey RM. Bacterial motility on a surface: many ways to a common goal. Annual review of microbiology. 2003;57:249-73.

27. Verstraeten N, Braeken K, Debkumari B, Fauvart M, Fransaer J, Vermant J, et al. Living on a surface: swarming and biofilm formation. Trends in microbiology. 2008;16(10):496-506.

28. Kearns DB. A field guide to bacterial swarming motility. Nature reviews Microbiology. 2010;8(9):634-44.

29. Wu Y, Jiang Y, Kaiser AD, Alber M. Self-organization in bacterial swarming: lessons from myxobacteria. Physical Biology. 2011;8(5):055003.

30. Howery KE, Şimşek E, Kim M, Rather PN. Positive autoregulation of the flhDC operon in Proteus mirabilis. Research in microbiology. 2018;169(4):199-204.

31. Little K, Austerman J, Zheng J, Gibbs KA. Cell Shape and Population Migration Are Distinct Steps of Proteus mirabilis Swarming That Are Decoupled on High-Percentage Agar. J Bacteriol. 2019;201(11):e00726-18.

32. Furness RB, Fraser GM, Hay NA, Hughes C. Negative feedback from a Proteus class II flagellum export defect to the flhDC master operon controlling cell division and flagellum assembly. J Bacteriol. 1997;179(17):5585-8.

33. Claret L, Hughes C. Functions of the subunits in the FlhD(2)C(2) transcriptional master regulator of bacterial flagellum biogenesis and swarming. Journal of molecular biology. 2000;303(4):467-78.

34. Deegan RD, Bakajin O, Dupont TF, Huber G, Nagel SR, Witten TA. Capillary flow as the cause of ring stains from dried liquid drops. Nature. 1997;389(6653):827-9.

35. Andac T, Weigmann P, Velu SKP, Pinçe E, Volpe G, Volpe G, et al. Active matter alters the growth dynamics of coffee rings. Soft Matter. 2019;15(7):1488-96.

36. Nellimoottil TT, Rao PN, Ghosh SS, Chattopadhyay A. Evaporation-induced patterns from droplets containing motile and nonmotile bacteria. Langmuir : the ACS journal of surfaces and colloids. 2007;23(17):8655-8.

37. Rieck VT, Palumbo SA, Witter LD. Glucose availability and the growth rate of colonies of Pseudomonas fluorescens. Journal of general microbiology. 1973;74(1):1-8.

38. Shao X, Mugler A, Kim J, Jeong HJ, Levin BR, Nemenman I. Growth of bacteria in 3-d colonies. PLoS computational biology. 2017;13(7):e1005679.

39. Warren MR, Sun H, Yan Y, Cremer J, Li B, Hwa T. Spatiotemporal establishment of dense bacterial colonies growing on hard agar. eLife. 2019;8:e41093.

40. Lavrentovich MO, Koschwanez JH, Nelson DR. Nutrient shielding in clusters of cells. Physical review E, Statistical, nonlinear, and soft matter physics. 2013;87(6):062703-.

41. Dal Co A, van Vliet S, Ackermann M. Emergent microscale gradients give rise to metabolic cross-feeding and antibiotic tolerance in clonal bacterial populations. Philosophical transactions of the Royal Society of London Series B, Biological sciences. 2019;374(1786):20190080.

42. Sternberg C, Christensen BB, Johansen T, Toftgaard Nielsen A, Andersen JB, Givskov M, et al. Distribution of bacterial growth activity in flow-chamber biofilms. Applied and environmental microbiology. 1999;65(9):4108-17.

43. Clemmer KM, Rather PN. Regulation of flhDC expression in Proteus mirabilis. Research in microbiology. 2007;158(3):295-302.

44. Howery KE, Clemmer KM, Rather PN. The Rcs regulon in Proteus mirabilis: implications for motility, biofilm formation, and virulence. Current Genetics. 2016;62(4):775-89.

45. Howery KE, Clemmer KM, Şimşek E, Kim M, Rather PN. Regulation of the Min Cell Division Inhibition Complex by the Rcs Phosphorelay in Proteus mirabilis. J Bacteriol. 2015;197(15):2499-507.

46. Wang Q, Zhao Y, McClelland M, Harshey RM. The RcsCDB Signaling System and Swarming Motility in Salmonella enterica Serovar Typhimurium: Dual Regulation of Flagellar and SPI-2 Virulence Genes. J Bacteriol. 2007;189(23):8447-57.

47. Samanta P, Clark ER, Knutson K, Horne SM, Prüß BM. OmpR and RcsB abolish temporal and spatial changes in expression of flhD in Escherichia coli biofilm. BMC microbiology. 2013;13:182.

48. Girgis HS, Liu Y, Ryu WS, Tavazoie S. A Comprehensive Genetic Characterization of Bacterial Motility. PLoS genetics. 2007;3(9):e154.

49. Francez-Charlot A, Laugel B, Van Gemert A, Dubarry N, Wiorowski F, Castanié-Cornet MP, et al. RcsCDB His-Asp phosphorelay system negatively regulates the flhDC operon in Escherichia coli. Molecular microbiology. 2003;49(3):823-32.

50. Huang YH, Ferrières L, Clarke DJ. The role of the Rcs phosphorelay in Enterobacteriaceae. Research in microbiology. 2006;157(3):206-12.

51. Majdalani N, Gottesman S. The Rcs phosphorelay: a complex signal transduction system. Annual review of microbiology. 2005;59:379-405.

52. Kaiser D. Bacterial Swarming: A Re-examination of Cell-Movement Patterns. Current Biology. 2007;17(14):R561-R70.

53. Inoue T, Shingaki R, Hirose S, Waki K, Mori H, Fukui K. Genome-Wide Screening of Genes Required for Swarming Motility in Escherichia coli K-12. J Bacteriol. 2007;189(3):950-7.

54. Dong T, Joyce C, Schellhorn H. The Role of RpoS in Bacterial Adaptation. In: El-Sharoud W, editor. Bacterial Physiology: Springer Berlin Heidelberg; 2008. p. 313-37.

55. Phaiboun A, Zhang Y, Park B, Kim M. Survival Kinetics of Starving Bacteria Is Biphasic and Density-Dependent. PLoS computational biology. 2015;11(4):e1004198.

56. Majdalani N, Hernandez D, Gottesman S. Regulation and mode of action of the second small RNA activator of RpoS translation, RprA. Molecular microbiology. 2002;46(3):813-26.

57. Peterson CN, Carabetta VJ, Chowdhury T, Silhavy TJ. LrhA regulates rpoS translation in response to the Rcs phosphorelay system in Escherichia coli. J Bacteriol. 2006;188(9):3175-81.

58. Lok T, Overdijk O, Piersma T. The cost of migration: spoonbills suffer higher mortality during trans-Saharan spring migrations only. Biology Letters. 2015;11(1):20140944.

59. Flack A, Fiedler W, Blas J, Pokrovsky I, Kaatz M, Mitropolsky M, et al. Costs of migratory decisions: A comparison across eight white stork populations. Sci Adv. 2016;2(1):e1500931-e.

60. Rankin MA, Burchsted JCA. The Cost of Migration in Insects. Annual Review of Entomology. 1992;37(1):533-59.

61. van Ditmarsch D, Boyle KE, Sakhtah H, Oyler JE, Nadell CD, Déziel É, et al. Convergent evolution of hyperswarming leads to impaired biofilm formation in pathogenic bacteria. Cell Rep. 2013;4(4):697-708.

62. Ferrières L, Clarke DJ. The RcsC sensor kinase is required for normal biofilm formation in Escherichia coli K-12 and controls the expression of a regulon in response to growth on a solid surface. Molecular microbiology. 2003;50(5):1665-82.

63. Guttenplan SB, Kearns DB. Regulation of flagellar motility during biofilm formation. FEMS microbiology reviews. 2013;37(6):849-71.

Figure legends

Figure 1. Different migration pattern of WT and Δ*rcsC* strains. (A) WT colony 7 hr after inoculation. (B) Δ*rcsC* colony 6 hr after inoculation. Note that a Δ*rcsC* colony begins colony expansion ~1 hr earlier than a WT colony. Purple-line zones indicate the original inoculum area. (C) Percentage of migratory cells. Error bars indicate one standard deviation from two independent experiments. ~800 cells were analyzed in each experiment. See Materials and Methods, and Supplementary Fig. 2 for the detail of experiments and analyses.

Figure 2. Characterizing spatio-temporal regulation of cell motility. (A) Phase contrast and fluorescence images of a WT micro-colony right before the onset of migration (~6 hr after inoculation). A $P_{flhDC} - gfp$ transcriptional fusion construct was used. See Supplementary Fig. 8 for Δ*rcsC* micro-colony images. (B-D) *flhDC* expression at the colony center. GFP intensities in the centroid of the colony and its four nearest-neighbor pixels were averaged and normalized by the mean GFP intensity of the entire colony. (E) *flhDC* expression away from the colony center. The colony radius (r) was identified, and *flhDC* expression at $0.6 \times r$ was averaged and normalized by the mean GFP intensity of the entire colony. See Supplementary Fig. 9 for a similar plot of *flhDC* expression beyond $0.6 \times r$. Two independent

experiments were performed. In each experiment, ~10 colonies were analyzed. Error bars indicate one standard deviation from the two independent experiments.

Figure 3. $P_{flhDC}-gfp$ expression in liquid cultures and the fitness effect of Rcs. (A) *flhDC* expression in liquid cultures. (B) Biomass ($OD_{600}\times$ ml) and cell viability (CFU). For each data set, measured values were normalized by the value of WT at the first time point. WT biomass data (open green circles) are not clearly visible in some cases because they overlapped with viability data (solid green circles). Error bars represent standard deviation from two independent experiments.

Figure 1

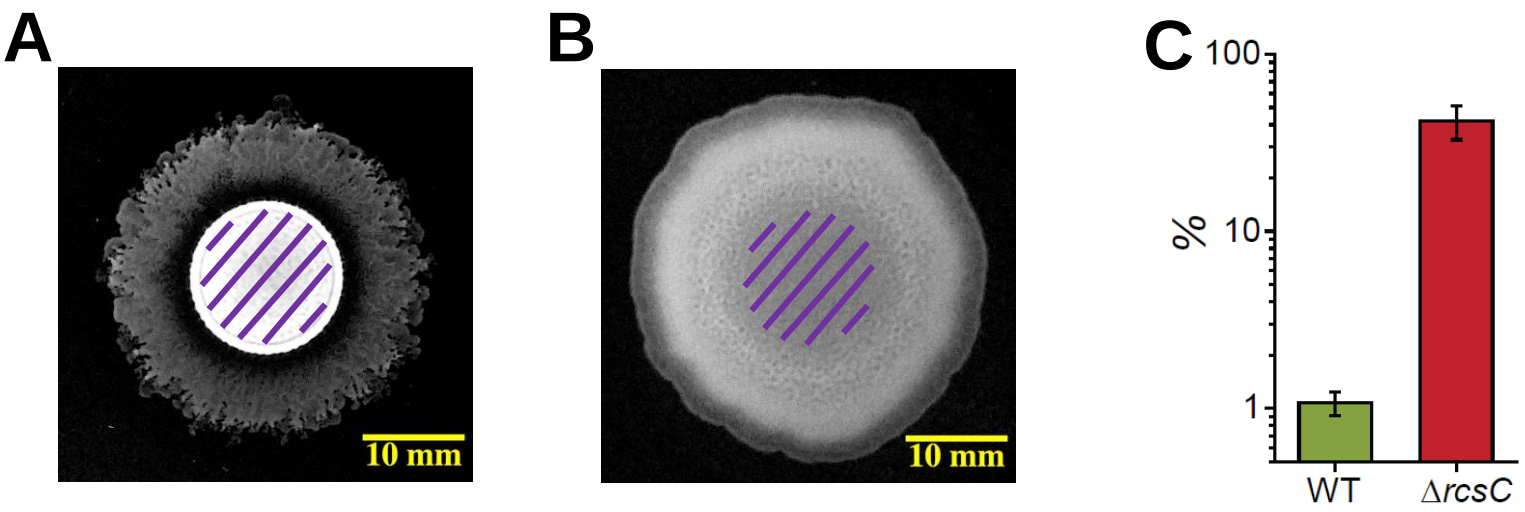

Figure 2

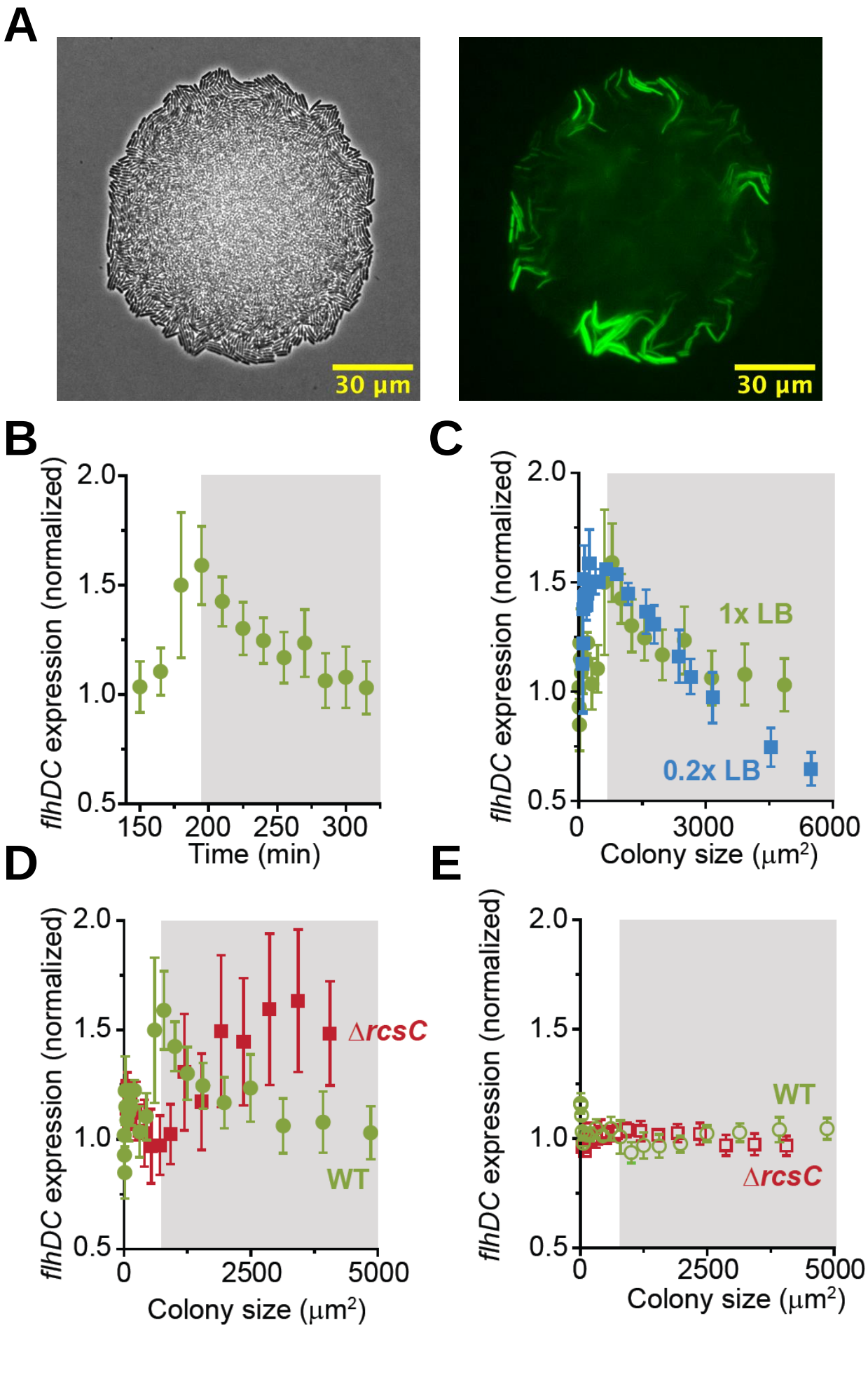
A
30 µm
30 µm
B
flhDC expression (normalized)
2.0
1.5
1.0
0.5
150
200
250
300
Time (min)
C
flhDC expression (normalized)
1x LB
0.2x LB
0
3000
6000
Colony size (µm²)
D
flhDC expression (normalized)
ΔrcsC
WT
0
2500
5000
Colony size (µm²)
E
flhDC expression (normalized)
WT
ΔrcsC
0
2500
5000
Colony size (µm²)

Figure 3

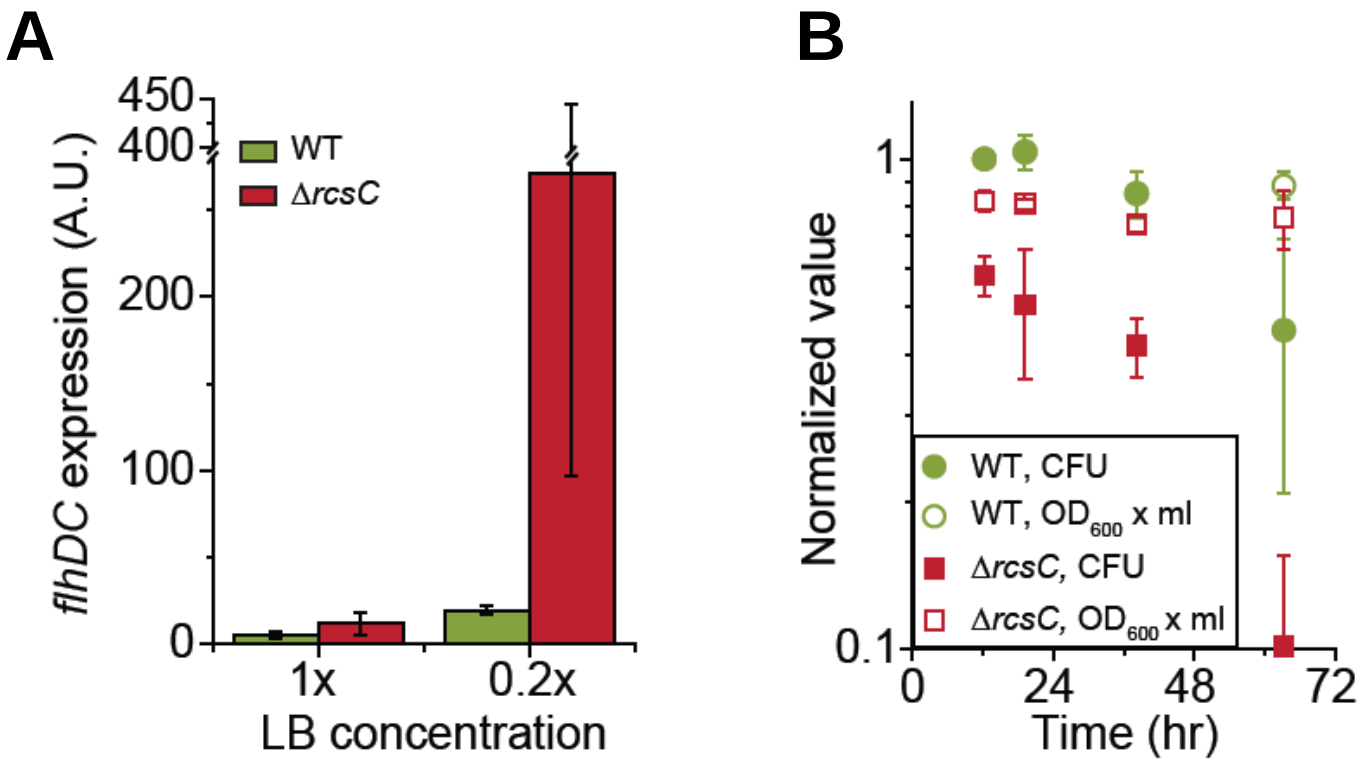
A
450
400
200
100
0
WT
ΔrcsC
flhDC expression (A.U.)
1x
0.2x
LB concentration
B
1
0.1
Normalized value
WT, CFU
WT, OD600 x ml
ΔrcsC, CFU
ΔrcsC, OD600 x ml
0
24
48
72
Time (hr)